Brief Communication: Precision measurement of the index of refraction of deep glacial ice at radio frequencies at Summit Station, Greenland

Christoph Welling[1] and The RNO-G Collaboration [*]

[1]Dept. of Physics, Enrico Fermi Inst., Kavli Inst. for Cosmological Physics, University of Chicago, Chicago, IL 60637, USA
[*]A full list of authors appears at the end of the paper.

Correspondence: Christoph Welling (christophwelling@uchicago.edu, authors@rno-g.org)

Abstract. Glacial ice is used as a target material for the detection of ultra-high energy neutrinos, by measuring the radio signals that are emitted when those neutrinos interact in the ice . Thanks to the large attenuation length We report on the measurement of the index of refraction of glacial ice at radio frequencies , these signals can be detected over distances of several kilometers. One experiment taking advantage of this is at Summit Station, Greenland. This measurement is of particular importance for the Radio Neutrino Observatory Greenland(RNO-G), , an experiment currently under construction at Summit Station, near the apex of the Greenland icesheet. These experiments require a thorough understanding of the dielectric properties of ice at radio frequencies. Towards this goal, calibration campaigns have been undertaken at Summit, during which we recorded radio reflections off internal layers in the that seeks to detect radio signals from ultra-high energy neutrino interactions in the icesheet. Using data from the nearby GISP2 and GRIP ice cores, we show that these reflectors can be associated . By correlating radio reflections in the bulk ice with features in the ice conductivity profiles; we use this connection to conductivity measurements from ice cores, we determine the index of refraction of the bulk ice as $n = 1.778 \pm 0.006$.

1 Introduction

The Radio Neutrino Observatory Greenland (RNO-G) is an experiment for the detection of ultra-high energy neutrinos (Aguilar et al., 2021), currently under construction near Summit Station, Greenland. It aims to discover the first astrophysical neutrinos with energies >10PeV through the measurement of via radio signals from particle showers that are produced by the interactions of neutrinos in glacial ice.

In order to use ice as a detection medium, a thorough knowledge of its dielectric properties at radio frequencies is necessary. To this end, a series of calibration campaigns has been undertaken at Summit Station, where RNO-G is located, and will continue in coming years. These included measurements of the ice attenuation length using the backscatter of radio signals off the bedrock (Aguilar et al., 2022a, c). In addition to the bedrock echo, reflections were also observed Doing so requires a good understanding of the optical properties of the ice at radio frequencies. We use the connection between radio echos from within the ice sheet. Radio reflectors in deep ice have been shown to result from dielectric contrast, such as an abrupt change and abrupt changes in ice conductivity. We want to use this connection between ice conductivity and reflectivity, demonstrated

at , which has been demonstrated for the site of the Greenland Ice Core Project (GRIP) (Hempel et al., 2000) , for a precision measurement of to measure the index of refraction of the bulk iceat the site of the RNO-G experiment, similar to the method employed by Winter et al. (2017). While the The index of refraction of glacial ice is relevant for radioglaciological surveys, it is of special importance for an experiment like RNO-G, since it determines the so-called ice plays an important role for the radio detection of neutrinos, specifically in determining the Cherenkov angle, which describes i.e. the direction into which the radio signal from a particle shower is emitted. It also sets a boundary condition for the index of refraction profile of the firn layer, which needs to be understood to reconstruct the arrival directions of the radio signals (Aguilar et al., 2022b), and influences the observable ice volume by creating a *shadow zone* from where signal propagation to the detector is suppressed (Barwick et al., 2018; Deaconu et al., 2018).

2 Radio Echo Measurements

The radio echo measurements used in this paper were carried out in the summer of 2022 at Summit Station, near the GISP2 borehole. They are a follow-up to measurements done in 2021 with the goal of measuring the radio attenuation of the ice (Aguilar et al., 2022a, c). The setup is almost identical to the previous one with the main changes change being the replacement of the log-periodic dipole antennas with horn antennas, whose smaller group delay leads to shorter radio pulses, and the measurements being taken near the GISP2 hole.

Signals were produced by an IDL-2 a pulse generator and split into two outputs. One output , one of which was used as a trigger signal. The other was fed into a 145MHz highpass filter and then into one of the horn antennasthrough an MILDTL17 and an LMR240 coaxial cable. The filter and the horn antenna's response restrict the radio , which together restrict the signal to a band of 145-500MHz , similar to the bandused by RNO-G. The other output, used as a trigger signal , was attenuated by 40 and fed into an oscilloscope via an MILDTL17, an LMR240 and an LMR400 cable. Both the transmitting and the receiving antenna were buried in the snow on opposing sides of the GISP2 hole, at about 51distance from the hole. The receiving antenna was connected to band. The signal from the receiving horn antenna was fed into an amplifier of the same type as used by the shallow component of an RNO-G station via a MILDTL17 coaxial cable, and connected from there to the oscilloscope with an LMR240 cable. Because the echo from a single radio pulse quickly falls below the noise backgroundand then recorded by an oscilloscope. Both antennas were placed on opposing sides of the GISP2 borehole, at a distance of about 51m from the hole. To reduce noise, 12000 individual waveforms were averagedand recorded at a sampling rate of 2.5 . The strong air-to-air signal between the antennas caused the amplifier to saturate, requiring some time to recover, making the first 2.6 not usable, and the radio echo falls below the noise background around 10.6 after the trigger, which sets the range of depths that are observable with this measurement.

Two additional . Additional radio echo measurements were taken about 550m to the north of the from the GISP2 hole, in the vicinity of the borehole, near the so-called "Bally Building". Signals were produced by an AVTECH AVIR-1-C pulse generator, and used the same antennas as (Aguilar et al., 2022c, a), which provides more output power and a faster trigger rate, but could not be used at the GISP2 hole because of a lack of a suitable power source. This setup allowed to average 30000 waveforms and

detect While the use of a more powerful pulser allowed us to observe radio reflections from deeper in the ice, but also caused more amplifier saturation. Therefore, another run was done with an additional 12 of attenuation at the transmitting antenna, which mitigated the saturation issue but also caused the sigal to fall below the noise floor sooner.

From each run, we calculate the return power of the radio signal in a sliding rectangular time window with a width of 10 , corresponding to roughly one period of the radio signal at the lowest frequency in the band. The result is shown in Fig. **??**. The radio signal power is then corrected for the propagation distance using the attenuation length measured in (Aguilar et al., 2022a) .[1]

The distance between the the distance from the GISP2 hole and the Bally building would introduce an unknown uncertainty on the reflector depths, so only the measurements taken directly at the GISP2 hole will be used to calculate the made the measurements unsuitable for the index of refraction . We will nevertheless show the measurements near the Bally building to demonstrate that the relation between radio reflections and conductivity measurement. They did, however, confirm that the observed correlation between radio reflectors and DEP data holds to greater depths. To combine measurements, the time offset between them is determined through cross-correlation and the return power is averaged where they overlap.

3 Index of Refraction Measurement

Top: AC conductivity data σ_{∞} from the GRIP ice core, adjusted to the corresponding depths at the GISP2 site, overlaid with the running mean of the conductivity. Bottom: Root mean square (RMS) of the deviation of the conductivity from the running mean.

The principle of

3 Index of Refraction Measurement

We measure the index of refraction measurement is as follows: Assuming that the observed radio echos are produced by abrupt changes in the conductivity of the ice, we can match these reflections to specific features in the ice core conductivity data and calculate the index of refraction as

$$n = \frac{c_0 \cdot \Delta t}{2 \cdot \Delta z}$$

where c_0 is the vacuum speed of light, Δt is the time between observed radio echos and Δz is the difference in depth of the reflectors. The of the bulk ice by associating radio echos with reflective layers identified at known depths through dielectric profiling (DEP). While the direct current conductivity of the GISP2 ice core has been measured for its entire depth range (Taylor, 2003), but the relevant property governing the effect on radio waves is the alternating current (AC)

[1] To convert the arrival time of the radio pulse to the propagated distance, an assumption about the index of refraction n and any time offsets ΔT due to e.g. cable delays already has to be made here. One could redo this correction for each value of n and ΔT, but this dramatically increases the computing demands. The choice of n and ΔT at this stage turns out to have a negligible impact on the final result, so we ignore this complication here.

conductivity σ_∞, which has not been determined for both the GISP2 . The AC conductivity has been measured using dielectric profiling for the nearby Greenland Ice Core Project (GRIP) core (Greenland Ice Core Project, 1994; Wolff et al., 1995). Both ice cores were taken only and the GRIP cores, alternating current conductivity measurements are only available from GRIP (Greenland Ice Core Project, 1994; Wolff et al., 1995), which is located roughly 28km apart, and from Summit. As the DC conductivity measurements are well correlated up to depths of 2700 (Taylor et al., 1993). Furthermore, radar surveys have shown that most internal reflectors are of both ice cores is very similar (Taylor et al., 1993), and most internal layers have been shown to be continuous between the GISP2 and GRIP drill sites , except for those close to the bedrock (Jacobel and Hodge, 1995). It is therefore reasonable to assume that the AC conductivity at GISP2 is similar to that at GRIP, though there are offsets between layer depths at the two sites, which we correct for based on (Rasmussen et al., 2014; Seierstad et al., 2014; Centre for Ice and Climate, Niels . two sites (Jacobel and Hodge, 1995), we use the DEP data from GRIP and correct for the difference in layer depths using (Rasmussen et al., 2014; Seierstad et al., 2014; Centre for Ice and Climate, Niels Bohr Institute, 2014).

For a given index of refraction, the signal return The relation between the layer depth z and the signal propagation time t can be converted to a reflector depth using

$$z = \frac{1}{2} \cdot \frac{c_0}{n} \cdot (t - \Delta T)$$

if the distance between transmitting and receiving antenna is negligible. If they are further apart, as is the case here, the additional travel distance is accounted for via the expression is given by

$$z = \sqrt{z_0^2 - 0.25 \cdot d^2}\frac{1}{2} \cdot \frac{c_0}{n} \cdot (t - \Delta T) \quad (1)$$

where d is the distance between the transmitting and receiving antennas, 102in our case. The changing c_0 is the vacuum speed of light, n is the index of refraction in the firn causes radio signals to be bent downward as they propagate, which causes a small change to the propagation time. We simulated this effect using the analytic raytracing method (Glaser et al., 2020) and found it to be less than 1, which is negligible.

and ΔT is a second free parameter which accounts as a free parameter used to account for time offsets due to cable delays, a changing the different index of refraction in the firn, and the unknown offset between the zero depth point of the GISP2 core and the location of the antennas . Our strategy to measure the index of refraction is to vary n and ΔT, convert the radio signal return times to the corresponding depths, and calculate the correlation between the ice conductivity at this depth and the return power. For depths between two conductivity measurements, the value is linearly interpolated between the two closest data points.

However, we do not directly correlate the AC conductivity with the radio echo power. Radio reflections at large depths are thought to be caused by abrupt changes in the AC conductivity a possible offset between our antennas and the 0m mark of the ice . Therefore, rate of change of σ_∞ is more important than the value of σ_∞ itself. We therefore average the core.

We average the ice conductivity over a sliding window with a width of 5m . We then sliding window and calculate the root mean square (RMS) of the difference between σ_∞ from this average squared of the deviation of the conductivity from this mean over a 2m sliding window , roughly equivalent to the as an indicator of the change in conductivity. We also correct our

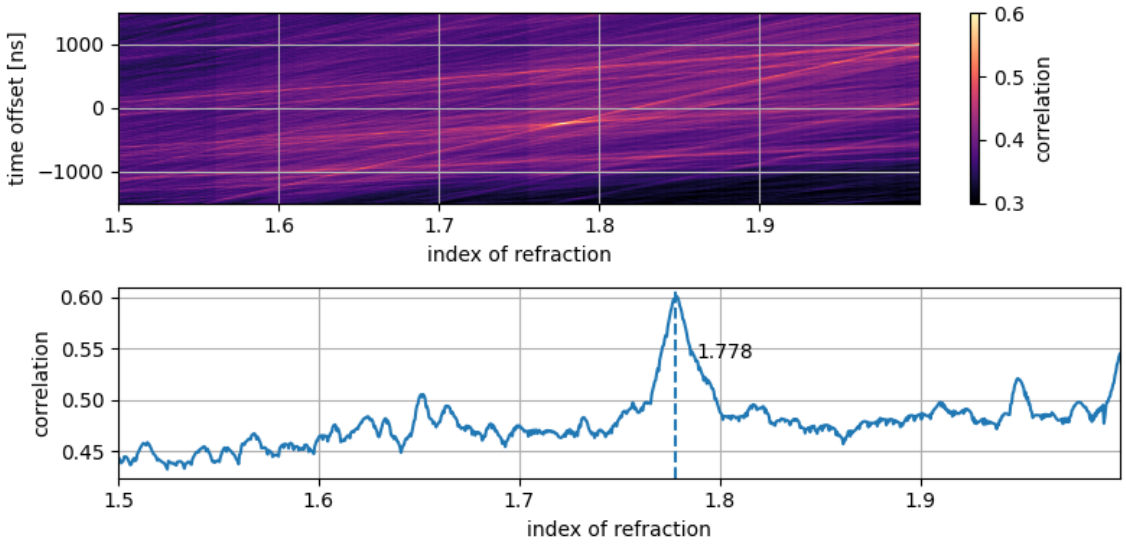

Figure 1. Top: Correlations between radio return power and RMS($\sigma_\infty - \sigma_{avg}$) for a given combination of index of refraction and time offset values. Bottom: Maximum correlation between radio return power and ice conductivity as a function of index of refraction.

radio echo measurements for signal attenuation using Aguilar et al. (2022a) and calculate the return power in a sliding 10ns windowover which the return power is averaged.The resulting plots for σ_∞ and RMS($\sigma_\infty - \sigma_{avg}$) are shown in Fig. **??**.

Top: Correlations between radio return power and RMS($\sigma_\infty - \sigma_{avg}$) for a given combination of index of refraction and time offset values. Bottom: Maximum correlation between radio return power and ice conductivity as a function of index of refraction. The time offset is left to vary for each value of n.

The resulting . The index of refraction is then determined by converting the return times to depths using Eq. 1 and calculating the correlation between radio return power and RMS($\sigma_\infty - \sigma_{avg}$) echo and conductivity data for different values of ΔT and n is shown in and ΔT.

The result (Fig. 1. It) shows a clear maximum at a value of $n = 1.778$.

Using this result, we plot Plotting the radio return power as a function of reflector depth along with ice conductivity. The result over the DEP measurements (Fig. 2) shows a good correlation between the two. Most jumps that most abrupt changes in conductivity are matched with a radio echo, though there are exceptions, most notably at 520. There are a few radio echos that do not seem to have a corresponding feature in the conductivity data, for example at 230 a few exceptions. Similar inconsistencies between radio reflections and ice conductivity DEP data and radio echos have also been noted by other measurements (Eisen et al., 2003).

Same plot as Fig. 2, but with

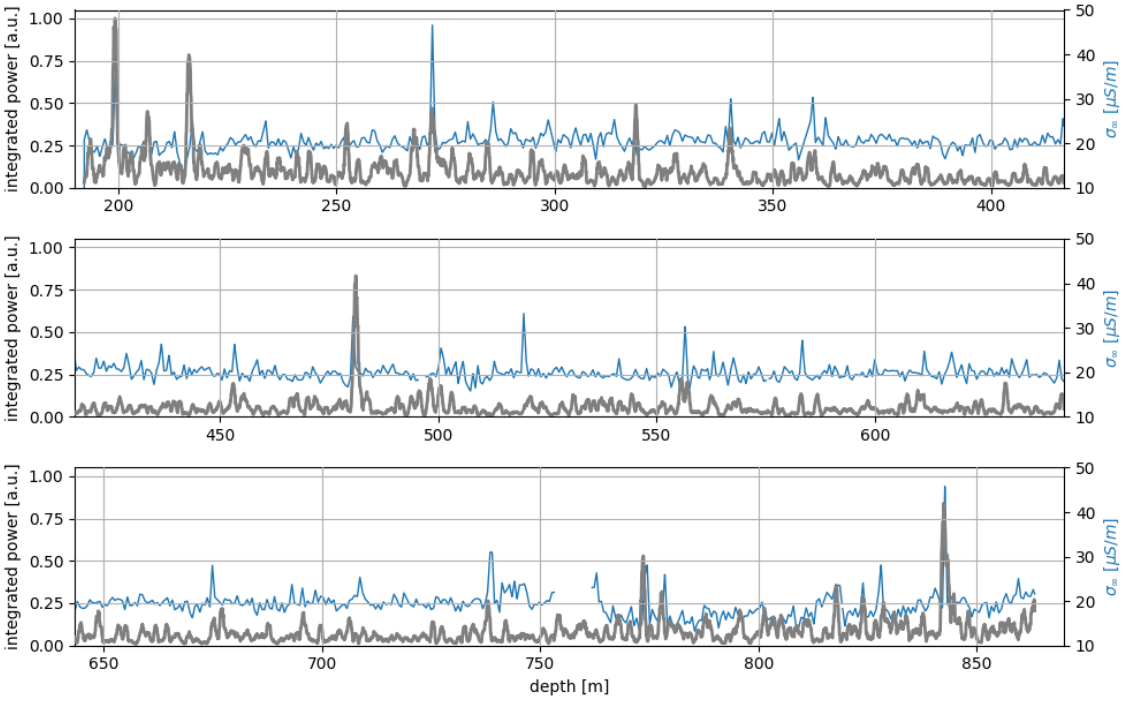

Figure 2. Radio return power as a function of the corresponding reflector depth, calculated using the reconstructed index of refraction n and time offset ΔT (~~solid~~ thick gray line), overlaid with the AC conductivity of the ice (~~dashed~~ thin blue line).

4 Uncertainty Estimation

The uncertainty of the ~~measurements near the Bally building included.~~

~~If we repeat this process with the combined measurements from all three runs, the result is very similar to the one obtained from using just the measurement at the GISP2 hole, with the maximum correlation for an index of refraction of $n = 1.774$. Superimposing the radio return power and the ice conductivity (Fig. **??**) shows that the correlation holds down to larger depths. As the deeper measurements were taken at a considerable distance from the GISP2 hole, there may be a change in the depths of some reflectors. The good fit between radio echos and σ_∞ suggests that this change is small, if present at all. Still, it represents a potentially significant and difficult to estimate uncertainty on the index of refraction measurement, which is why we prefer the measurement taken at the GISP2 hole itself. But it demonstrates that this~~ index of refraction measurement ~~can be extended to greater depths relatively easily, if desired.~~

5 ~~Uncertainty Estimation~~

~~As shown by Eq. **??**, the two primary types of uncertainty we need to consider are~~ consists of the uncertainties on the radio echo ~~return time, and the depth of the corresponding reflective layer.~~

propagation times and the depths of the associated reflective layers. The first radio reflectors used for this measurement are at a depth of roughly 200m, ~~which is~~ well below the transition between firn and ice, which occurs at 75-77m (Gow et al., 1997). ~~By including~~ Including a global time offset as a free parameter ~~, we are effectively only considering the time difference between reflections from different layers in the ice, so cable delays, the changing~~ removes uncertainties from the index of refraction ~~profile in the firn~~of the firn, cable delays and the height of the antennas relative to the 0m mark of the GISP2 ~~core can be ignored, as they affect the signal from each reflector~~ ice core, as these affect all reflectors equally. The ~~waveforms for each run were recorded on a single trace with a sampling rate of 2.5 , giving sub-nanosecond precision for the waveforms returning from different reflectors. The return power was integrated over a~~ dominant uncertainty on Δt is the 10ns window ~~, which we conservatively take as the uncertainty on Δt~~over which the return power was integrated. The first and ~~the last radio echo~~ last radio echos that can be clearly associated with a specific ~~peak in the ice conductivity~~ DEP feature are at about 2.5µs (195m) and 10.2µs(845m), ~~respectively,~~ resulting in a relative uncertainty of ~~$\sigma_t = 0.1\%$.~~ σ_t=0.1%.

The uncertainty on the depth of the GISP2 conductivity data is given as 2 to 3 m at 3 km (Greenland Ice Core Project, 1994). We take this as an upper limit, though over the ∼650 m range in depth we are looking at, the true uncertainty is likely much smaller. The uncertainty on the matching between the GISP2 and GRIP ice cores is given as 0.5 m ~~, except for some depths which are outside the range used in this measurement~~ (Seierstad et al., 2014). Thus, the conservative 2 m uncertainty on the GISP2 depth scale is the dominant uncertainty~~, which is equal to the 2 window over which $\mathrm{RMS}(\sigma_\infty - \sigma_{avg})$ was calculated~~. Over a depth range of 650m, this yields a relative uncertainty of $\sigma_z = 0.3\%$.

Quadratically adding the relative uncertainties on Δz and Δt results in a relative uncertainty of $\sigma_n = 0.3\%$, or $\sigma_{n,abs} = 0.006$ in absolute terms.

~~This is larger than the difference between our two measurements of n, so even without knowing the uncertainty on the measurements at the Bally building, we can say that they agree within uncertainties.~~

~~Glacial ice has been shown to have birefringent properties, leading to a polarization dependence of the wave velocity that is larger than the uncertainty on our measurement in several places in Greenland (Zeising et al., 2023; Gerber et al., 2022). We have investigated birefringence in the ice at Summit Station before (Aguilar et al., 2022c), and constrained the difference in propagation time between polarizations parallel and perpendicular to the direction of ice flow to 1.6 ± 3.3over the full thickness of the ice sheet. Based on this, we conclude that birefringence effects are negligible for our measurement.~~

~~The index of refraction of ice has also been shown to be temperature dependent (Fujita and Mae, 1994). Our measurement implicitly assumes a constant index of refraction over the entire depth range of the measurement. As the temperature profile of the GISP2 borehole is constant to within 1over the upper 2(Clow, 1999), this assumption is justified.~~

5 Conclusion and Outlook

We report on the observation of reflective layers in the ice sheet near Summit Station, Greenland and compare them to conductivity measurements from the ~~GISP2 and GRIP ice cores~~GRIP ice core. We show that ~~certain~~ most radio echos can be attributed to features in the ice conductivity, and use this relationship to measure the index of refraction of the bulk ice as

$n = 1.778 \pm 0.006$. Though the available equipment limited our measurement to the upper ~850of the ice sheet, we show that the relation between ice conductivity and radio reflections should hold to much greater depths. This would allow to easily extend this measurement and improve on its accuracy in the future. An extension these radio echo measurements, with a wider frequency response, could, in principle, also correlate the characteristics of the observed radar echoes with the known GISP2 ice chemistry.

Acknowledgements. We are thankful to the staff at Summit Station for supporting our deployment work in every way possible. Also to our colleagues from the British Antarctic Survey for embarking on the journey of building and operating the BigRAID drill for our project.

We would like to acknowledge our home institutions and funding agencies for supporting the RNO-G work; in particular the Belgian Funds for Scientific Research (FRS-FNRS and FWO) and the FWO programme for International Research Infrastructure (IRI), the National Science Foundation (NSF Award IDs 2118315, 2112352, 211232, 2111410) and the IceCube EPSCoR Initiative (Award ID 2019597), the German research foundation (DFG, Grant NE 2031/2-1), the Helmholtz Association (Initiative and Networking Fund, W2/W3 Program), the University of Chicago Research Computing Center, and the European Research Council under the European Unions Horizon 2020 research and innovation programme (grant agreement No 805486).

Team List

Juan A. Aguilar[1], Patrick Allison[2], Dave Z. Besson[3], Abigail Bishop[4], Olga Botner[5], Sjoerd Bouma [6], Stijn Buitink[7], Whitmaur Castiglioni[8], Maddalena Cataldo[6], Brian A. Clark[9], Alan Coleman[5], Kenneth Couberly[3], Zachary Curtis-Ginsberg[4], Paramita Dasgupta[1], Simon de Kockere[10], Krijn D. de Vries[10], Cosmin Deaconu[8], Michael A. DuVernois[4], Anna Eimer[6], Christian Glaser[5], Allan Hallgren[5], Steffen Hallmann[11], Jordan C. Hanson[12], Bryan Hendricks[13], Jacob Henrichs[11,6], Nils Heyer[5], Christian Hornhuber[3], Kaeli Hughes[8,13], Timo Karg[11], Albrecht Karle[4], John L. Kelley[4], Michael Korntheuer[1], Marek Kowalski[11,14], Ilya Kravchenko[15], Ryan Krebs[13], Robert Lahmann[6], Paul Lehmann[6], Uzair Latif[10], Philipp Laub[6], Chao-Hsuan Liu[15] Joseph Mammo[15], Matthew J. Marsee[16], Zachary S. Meyers[11,6], Kelli Michaels[8], Katahrine Mulrey[17], Marco Muzio[13], Anna Nelles[11,6], Alexander Novikov[18], Alisa Nozdrina[3], Eric Oberla[8], Bob Oeyen[19], Ilse Plaisier[6,11], Noppadol Punsuebsay[18], Lilly Pyras[11,6], Dirk Ryckbosch[19], Felix Schlüter[1], Olaf Scholten[10,20], David Seckel[18], Mohammad F. H. Seikh[3], Daniel Smith[8], Jethro Stoffels[10], Daniel Southall[8], Karen Terveer[6], Simona Toscano[6], Delia Tosi[4], Dieder J. Van Den Broeck[10,7], Nick van Eijndhoven[10], Abigail G. Vieregg[8], Janna Z. Vischer[6], Christoph Welling[8], Dawn R. Williams[16], Stephanie Wissel[13], Robert Young[3], Adrian Zink[6]

[1] Université Libre de Bruxelles, Science Faculty CP230, B-1050 Brussels, Belgium

[2] Dept. of Physics, Center for Cosmology and AstroParticle Physics, Ohio State University, Columbus, OH 43210, USA

[3] University of Kansas, Dept. of Physics and Astronomy, Lawrence, KS 66045, USA

[4] Wisconsin IceCube Particle Astrophysics Center (WIPAC) and Dept. of Physics, University of Wisconsin-Madison, Madison, WI 53703, USA

[5] Uppsala University, Dept. of Physics and Astronomy, Uppsala, SE-752 37, Sweden

[6] Erlangen Center for Astroparticle Physics (ECAP), Friedrich-Alexander-University Erlangen-Nürnberg, 91058 Erlangen, Germany

[7] Vrije Universiteit Brussel, Astrophysical Institute, Pleinlaan 2, 1050 Brussels, Belgium

[8] Dept. of Physics, Enrico Fermi Inst., Kavli Inst. for Cosmological Physics, University of Chicago, Chicago, IL 60637, USA

[9] Department of Physics, University of Maryland, College Park, MD 20742, USA

[10] Vrije Universiteit Brussel, Dienst ELEM, B-1050 Brussels, Belgium

[11] Deutsches Elektronen-Synchrotron DESY, Platanenallee 6, 15738 Zeuthen, Germany

[12] Whittier College, Whittier, CA 90602, USA

[13] Dept. of Physics, Dept. of Astronomy & Astrophysics, Penn State University, University Park, PA 16801, USA

[14] Institut für Physik, Humboldt-Universität zu Berlin, 12489 Berlin, Germany

[15] Dept. of Physics and Astronomy, Univ. of Nebraska-Lincoln, NE, 68588, USA

[16] Dept. of Physics and Astronomy, University of Alabama, Tuscaloosa, AL 35487, USA

[17] Dept. of Astrophysics/IMAPP, Radboud University, PO Box 9010, 6500 GL, The Netherlands

[18] Dept. of Physics and Astronomy, University of Delaware, Newark, DE 19716, USA

[19] Ghent University, Dept. of Physics and Astronomy, B-9000 Gent, Belgium

[20] Kapteyn Institute, University of Groningen, Groningen, The Netherlands

References

Aguilar, J. et al.: In situ, broadband measurement of the radio frequency attenuation length at Summit Station, Greenland, Journal of Glaciology, https://doi.org/10.1017/jog.2022.40, 2022a.

Aguilar, J. A. et al.: Design and Sensitivity of the Radio Neutrino Observatory in Greenland (RNO-G), JINST, 16, P03 025, https://doi.org/10.1088/1748-0221/16/03/P03025, 2021.

Aguilar, J. A. et al.: Reconstructing the neutrino energy for in-ice radio detectors: A study for the Radio Neutrino Observatory Greenland (RNO-G), Eur. Phys. J. C, 82, 147, https://doi.org/10.1140/epjc/s10052-022-10034-4, 2022b.

Aguilar, J. A. et al.: Radiofrequency Ice Dielectric Measurements at Summit Station, Greenland, https://doi.org/10.48550/arXiv.2212.10285, 2022c.

Barwick, S. W. et al.: Observation of classically 'forbidden' electromagnetic wave propagation and implications for neutrino detection, JCAP, 07, 055, https://doi.org/10.1088/1475-7516/2018/07/055, 2018.

Centre for Ice and Climate, Niels Bohr Institute: https://www.iceandclimate.nbi.ku.dk/data, accessed:2023-01-04, 2014.

Clow, G. D.: GISP2-D Temperature, https://doi.org/10.1594/PANGAEA.55517, 1999.

Deaconu, C., Vieregg, A. G., Wissel, S. A., Bowen, J., Chipman, S., Gupta, A., Miki, C., Nichol, R. J., and Saltzberg, D.: Measurements and Modeling of Near-Surface Radio Propagation in Glacial Ice and Implications for Neutrino Experiments, Phys. Rev. D, 98, 043 010, https://doi.org/10.1103/PhysRevD.98.043010, 2018.

Eisen, O., Wilhelms, F., Nixdorf, U., and Miller, H.: Identifying isochrones in GPR profiles from DEP-based forward modeling, Annals of Glaciology, 37, 344–350, https://doi.org/10.3189/172756403781816068, 2003.

Fujita, S. and Mae, S.: Causes and nature of ice-sheet radio-echo internal reflections estimated from the dielectric properties of ice, Annals of Glaciology, 20, 80–86, https://doi.org/10.3189/1994AoG20-1-80-86, 1994.

Gerber, T., Lilien, D., Rathmann, N., Franke, S., Young, T. J., Valero-Delgado, F., Ershadi, R., Drews, R., Zeising, O., Humbert, A., Stoll, N., Weikusat, I., Grinsted, A., Hvidberg, C., Jansen, D., Miller, H., Helm, V., Steinhage, D., O'Neill, C., and Eisen, O.: Crystal fabric anisotropy causes directional hardening of the Northeast Greenland Ice Stream, https://doi.org/10.21203/rs.3.rs-1812870/v1, 2022.

Glaser, C. et al.: NuRadioMC: Simulating the radio emission of neutrinos from interaction to detector, Eur. Phys. J. C, 80, 77, https://doi.org/10.1140/epjc/s10052-020-7612-8, 2020.

Gow, A. J., Meese, D. A., Alley, R. B., Fitzpatrick, J. J., Anandakrishnan, S., Woods, G. A., and Elder, B. C.: Physical and structural properties of the Greenland Ice Sheet Project 2 ice core: A review, Journal of Geophysical Research: Oceans, 102, 26 559–26 575, https://doi.org/https://doi.org/10.1029/97JC00165, 1997.

Greenland Ice Core Project: ftp://ftp.ncdc.noaa.gov/pub/data/paleo/icecore/greenland/summit/grip/, 1994.

Hempel, L., Thyssen, F., Gundestrup, N., Clausen, H. B., and Miller, H.: A comparison of radio-echo sounding data and electrical conductivity of the GRIP ice core, Journal of Glaciology, 46, 369–374, https://doi.org/10.3189/172756500781833070, 2000.

Jacobel, R. W. and Hodge, S. M.: Radar internal layers from the Greenland Summit, Geophysical Research Letters, 22, 587–590, https://doi.org/10.1029/95GL00110, 1995.

Rasmussen, S. O. et al.: A stratigraphic framework for abrupt climatic changes during the Last Glacial period based on three synchronized Greenland ice-core records: refining and extending the INTIMATE event stratigraphy, Quaternary Science Reviews, 106, 14–28, https://doi.org/https://doi.org/10.1016/j.quascirev.2014.09.007, 2014.

Seierstad, I. K. et al.: Consistently dated records from the Greenland GRIP, GISP2 and NGRIP ice cores for the past 104 ka reveal regional millennial-scale δ18O gradients with possible Heinrich event imprint, Quaternary Science Reviews, 106, 29–46, https://doi.org/https://doi.org/10.1016/j.quascirev.2014.10.032, 2014.

Taylor, K. C.: GISP2 Electrical conductivity measurements (Core D), https://doi.org/10.1594/PANGAEA.115684, 2003.

Taylor, K. C. et al.: Electrical conductivity measurements from the GISP2 and GRIP Greenland ice cores, Nature, 366, 549–553, https://doi.org/10.1038/366549a0, 1993.

Winter, A., Steinhage, D., Arnold, E. J., Blankenship, D. D., Cavitte, M. G. P., Corr, H. F. J., Paden, J. D., Urbini, S., Young, D. A., and Eisen, O.: Comparison of measurements from different radio-echo sounding systems and synchronization with the ice core at Dome C, Antarctica, The Cryosphere, 11, 653–668, https://doi.org/10.5194/tc-11-653-2017, 2017.

Wolff, E. W., Moore, J. C., Clausen, H. B., Hammer, C. U., Kipfstuhl, J., and Fuhrer, K.: Long-term changes in the acid and salt concentrations of the Greenland Ice Core Project ice core from electrical stratigraphy, Journal of Geophysical Research: Atmospheres, 100, 16 249–16 263, https://doi.org/https://doi.org/10.1029/95JD01174, 1995.

Zeising, O., Gerber, T. A., Eisen, O., Ershadi, M. R., Stoll, N., Weikusat, I., and Humbert, A.: Improved estimation of the bulk ice crystal fabric asymmetry from polarimetric phase co-registration, The Cryosphere, 17, 1097–1105, https://doi.org/10.5194/tc-17-1097-2023, 2023.